NANO LETTERS
Letter
Cite This: Nano Lett. 2019, 19, 1460−1466
pubs.acs.org/NanoLett

Electronic Stability of Carbon Nanotube Transistors Under Long-Term Bias Stress

Steven G. Noyce,[†] James L. Doherty,[†] Zhihui Cheng,[†] Hui Han,[‡] Shane Bowen,[‡] and Aaron D. Franklin*[,†,§]

[†]Department of Electrical & Computer Engineering, Duke University, Durham, North Carolina 27708, United States
[‡]Illumina Inc., 5200 Illumina Way, San Diego, California 92122, United States
[§]Department of Chemistry, Duke University, Durham, North Carolina 27708, United States

Supporting Information

ABSTRACT: Thousands of reports have demonstrated the exceptional performance of sensors based on carbon nanotube (CNT) transistors, with promises of transformative impact. Yet, the effect of long-term bias stress on individual CNTs, critical for most sensing applications, has remained uncertain. Here, we report bias ranges under which CNT transistors can operate continuously for months or more without degradation. Using a custom characterization system, the impacts of defect formation and charge traps on the stability of CNT-based sensors under extended bias are determined. In addition to breakdown, which is well-known, we identify three additional operational modes: full stability, slow decay, and fast decay. We identify a current drift behavior that reduces dynamic range by over four orders of magnitude but is avoidable with appropriate sensing modalities. Identification of these stable operation modes and limits for nanotube-based sensors addresses concerns surrounding their development for a myriad of sensing applications.

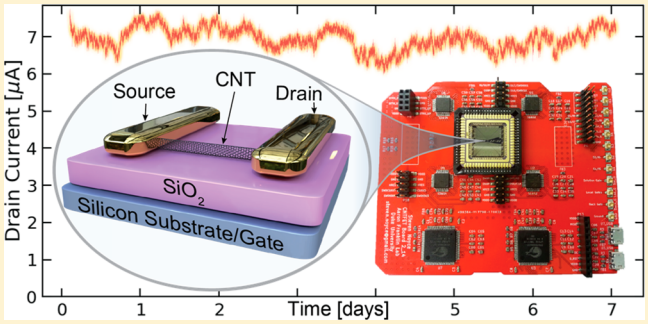

KEYWORDS: *Carbon nanotube, sensor, stability, bias stress, operating modes, settling*

Carbon nanotube-based sensors have received widespread attention for decades, with hundreds of papers on biosensors alone appearing within two years of the first nanotube device.[1−3] Since then, there have been numerous demonstrations of sensors that make use of nanotubes as the semiconducting channel in a carbon nanotube field-effect transistor (CNTFET), such as gas sensors,[4−7] protein concentration sensors,[8−11] antibody-based biosensors,[12−15] single-molecule time-response biosensors,[16−18] DNA sensors,[19−21] and many others.[16,22,23] Despite this strong research activity, the field still lacks fundamental understanding of how CNTFETs respond when operated under bias stress conditions relevant to many sensor applications, including long periods in the on-state, reacting to periodic gate voltage sweeps, or responding to intermittent application and removal of voltage.

The effects of bias stress have been studied for thin-film CNT network devices,[24−27] but with the exception of reports characterizing CNTFET breakdown,[28] little has been done to explore bias stress for CNTFETs with channels of one or a few parallel CNTs. The studies that report bias stress results for CNT thin-film devices have focused primarily on gate bias stress,[26] rather than the combination of gate and drain bias stress which is applicable to most device applications. Further, these studies have observed gate bias stress effects over periods of hours,[27] a time period comparable to the operating lifetime of some one-time use sensors, but shorter than the intended operating period of many sensor applications.

Literature reporting continuous operation of a CNTFET for more than a few hours is sparse.[24,25,27,29] Some studies indicate stability on the basis of infrequent/intermittent measurements or reported data spanning hours or less;[30] meanwhile, others have reported considerable instabilities related to nanotube breakdown, degradation, reactivity, large threshold voltage shifts, and so on.[31−33] Passivation of a CNT channel has been shown to make devices more robust,[33] but does not eliminate the possibility of electrically induced degradation, especially under varying ambient conditions in which many sensors explicitly require the nanotube to be exposed. This lack of published data demonstrating the effects of bias stress on CNTFETs over long time scales is an obstacle to the field. With companies such as Sensigent, C_2Sense, Nanōmix, and Alpha Szensor pursuing commercialization of CNT-based sensors and many groups seeking to demonstrate novel sensor morphologies, published long-term data should be available to guide and catalyze these efforts.

Received: October 4, 2018
Revised: January 1, 2019
Published: February 5, 2019

DOI: 10.1021/acs.nanolett.8b03986
Nano Lett. 2019, 19, 1460−1466

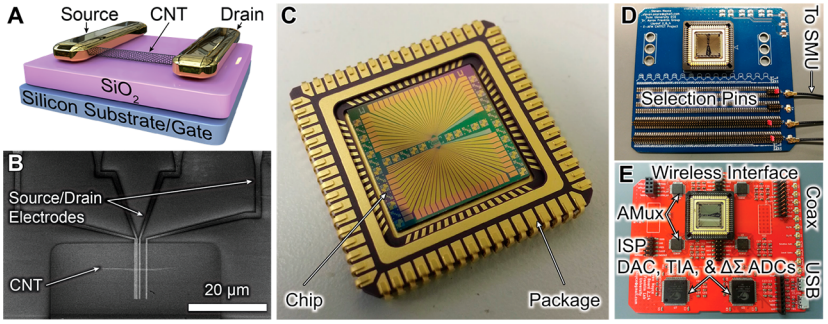

Figure 1. CNTFET structure, chip packaging, and custom measurement system. (A) CNTFET schematic with Pd source/drain contacts, 90 nm SiO_2 gate dielectric. (B) Scanning electron microscopy (SEM) image of a device set. (C) Photo of a CNTFET chip with 64 devices packaged for testing. (D) Photo of custom PCB with manual device selection and electrical characterization using precision SMUs. (E) Photo of fully automated PCB measurement platform: stand-alone, wireless, and programmable.

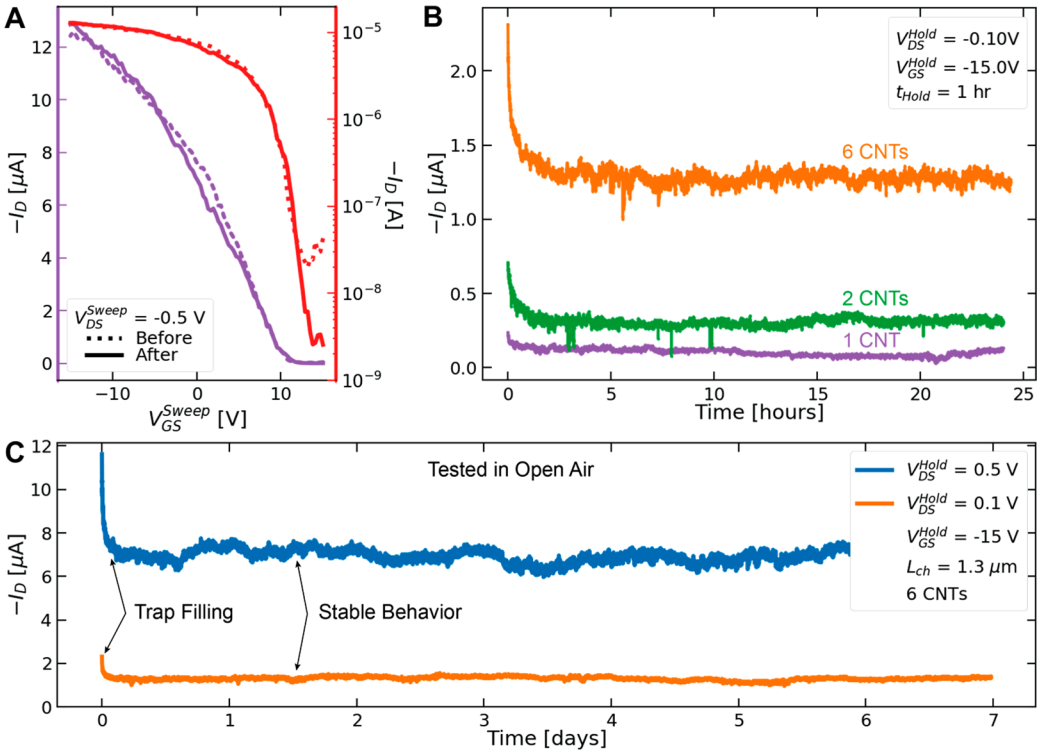

Figure 2. Long-term characterization of multiple CNTFET devices using custom PCB with SMUs. (A) Initial and final subthreshold and transfer characteristics of a device biased for a week. (B) Comparison of drain current stability over 24 h for devices with different numbers of CNTs in the channel. (C) Drain current of same device for two separate weeks under distinct drain voltages V_{DS}^{Hold} and a common gate voltage V_{GS}^{Hold}. A relatively steady state was observed under both bias conditions after initial stabilization of trap state occupancy.

The lack of long-term testing of CNTFETs is due, in part, to the traditional testing apparatus used to characterize CNTFET devices. Probe stations and semiconductor device analyzers are typically utilized together when characterizing CNTFETs. These systems are normally shared resources with high demand, such that it is uncommon for one experiment to have the opportunity of monopolizing both pieces of equipment for weeks at a time. Additionally, micromanipulators are susceptible to mechanical vibrations and temperature variations,[34] both of which can compromise the contact quality at some point during an extended test. What is needed is the ability to perform long-term characterization of CNTFETs without variability from the characterization setup, so that the specific stability of the carbon nanotubes can be examined.

For this study, we developed a measurement platform that allows for robust, long-term testing of many CNTFETs concurrently in a fully automated manner. This enabled investigation of the time response of CNTFETs under various sensor-relevant conditions, including long-term bias stress, intermittent bias stress, and periodic voltage sweeps. We demonstrate stable operation of CNTFETs in air for weeks, while also demarking voltage zones that lead to stability, slow decay (days), fast decay (hours), and failure. These results show that trap fill rates can cause large signal drift and a reduction in dynamic range from 83 to 6 dB when sensors rely on static drain current readings, necessitating specific measurement approaches to avoid these limitations.

The device structure used in this work was chosen to be similar to the majority of previously studied CNT-based sensors (Figures 1A and B) so that the results may have close applicability to the field as a whole. The fabrication process used loosely follows common fabrication methods,[28,35−39] with

DOI: 10.1021/acs.nanolett.8b03986
Nano Lett. 2019, 19, 1460−1466

all fabrication and characterization procedure details included in the Supporting Information (Figures S1−S4).

As discussed previously, the traditional test setup used to characterize CNTFET devices is not well-suited for long-term testing. To circumvent the issues with the traditional setup, the CNTFET chips were secured in ceramic packages using silver epoxy, and wire-bonds were formed to provide electrical connection between each device electrode and the pins of the chip package/carrier (Figure 1C). Once packaged, a chip was easily inserted into a 68-pin PLCC socket that provides extremely reliable contact to the devices and serves as an adapter from the relatively fragile contact pads to a variety of robust electrical connectors. Utilizing this socket, a custom printed circuit board (PCB) was designed to receive the packaged chip (Figure 1D) and connect to commercial source measure units (SMUs) for reliable and automated long-term testing.

The limiting resource in the setup described above is the costly and bulky precision SMUs. Bypassing the need for these SMUs would allow for many tests to be performed in parallel as device selection could be programmed and controlled remotely. Further, a standalone measurement PCB would allow for the characterization to be performed in diverse environments by simply relocating the hand-held board. These advantages, and others, were realized by designing a custom wireless PCB (Figure 1E). This board is able to apply up to 8 independent voltages, multiplex between devices, and measure currents as low as 10 pA. Complete descriptions of both measurement PCBs are available in the Supporting Information.

Utilizing the capabilities of these custom testing systems, long-term bias stress on CNTFETs was explored using static bias voltages V_{DS}^{Hold} (drain-source voltage) and V_{GS}^{Hold} (gate-source voltage), while dynamic voltages V_{DS}^{Sweep} and V_{GS}^{Sweep} were used to extract device metrics. After an initial settling time, devices exhibited stable performance in the on-state, even when biased continuously for a week at a moderate drain-source voltage V_{DS}^{Hold} = −0.5 V (~10^3 V/cm), as shown in Figures 2A and C. Because the devices were exposed to an open-air lab environment throughout the tests, most drift and noise in Figures 2B and C is attributed to changes in room temperature, adsorbates, and ambient lighting[40,41] (Figures S6−S8). This noise is relatively small (standard deviations of 83 nA and 294 nA with coefficients of variation of 6% and 4% at V_{DS}^{Hold} = 0.1 and 0.5 V, respectively) and no net change in current was observed after the initial settling period, exhibiting a reasonably steady state of operation at these particular bias conditions, an encouraging outcome for use of CNTFETs in sensors where the nanotube is exposed to a varying environment while under constant bias.

Prior to operating in the steady state, the CNTFETs presented a dramatic settling of the drain current (Figures 2B and C), almost halving the initial value, which occurred over the course of ~3 h regardless of the applied V_{DS}^{Hold} (Figure S9). This settling behavior is attributed to changes in trap state occupancy resulting from the applied gate bias.[24] Importantly, at the end of the week, the subthreshold and transfer characteristics of the device were reevaluated and found to be unaffected by the long-term bias stress (Figure 2A, also Figure S10 for more examples). Hence, the current settling behavior is a reversible rather than a permanent effect.

While the substantial settling of the current does not represent lasting degradation to the device, it is problematic for many potential sensor applications. If a sensor relies on drain current readings from intermittent applied bias, then this settling effect may cause a large drift in background current that could be misinterpreted as a sensing response. At the very least, it suggests that CNTFET-based sensors operated in this constant current-monitoring state would need to first be biased for long enough to reach the steady-state condition. However, many sensor applications are not able to tolerate "warm-up" stabilization times on the order of several hours. Pulsed measurements,[42] suspended nanotubes, and coated nanotubes[43] have all been proposed as solutions to this problem of charge traps, but each imposes additional restrictions on the operation or fabrication of the sensor.

As validation that charge traps are the primary source of the current settling, the devices could be reset by performing a full gate voltage sweep (from on- to off-state of the transistor and back again). After the full sweep, the current under a certain bias condition is nominally the same, regardless of any previous decay or settling. This gate-sweep-induced reset redistributes trapped charges, with the additional benefit of allowing the transfer characteristics of the device to be determined. The remainder of the experiments presented here employ these periodic reset sweeps of the gate voltage. We also found that grounding all device terminals for 30 s was an effective way to redistribute charges in trap states and reset the device without requiring a full gate voltage sweep; however, simply removing the applied voltages and allowing device terminals to float (no grounding and no applied bias) was not sufficient to enact a full reset (Figure S11). As with the gate voltage sweep, electrical grounding also redistributes charges that had filled trap states, but if the terminals are only allowed to float then reapplying the fixed bias condition leads to the device resuming its current decay behavior, indicative of charge traps that have remained filled/emptied and not reset. The effectiveness of these reset conditions supports the hypothesis that the observed current decay (Figures 2B and C) is due to bias-dependent trap states being filled or emptied of charge.

The efficacy of the device reset is seen in Figure 3A, where static bias conditions were interspersed with periodic gate sweeps, yielding a series of settling-followed-by-stabilization curves. The static bias (V_{DS}^{Hold} and V_{GS}^{Hold}) was held for intervals t_{Hold} = 6 h, with the set of subthreshold curves (Figure 3B) obtained between each interval. Although it takes more than an hour for the biased devices to reach steady state, this effect can still be observed in CNTFETs biased for only a few minutes at a time, as in Figure 3C. Throughout this entire process, the off-state (Figure 3B) and on-state (Figure 3D) remain unaffected, showing there is no lasting change to the device.

It has been shown previously that CNT current settling curves can be modeled by a sum of three exponentials with distinct settling rates.[29] As a result, curves like those shown in Figures 3A and C were fit to triexponential models, as shown in Figure S12. The three settling rates were found to be on the order of 30, 1000, and 7000 s for all devices studied, with the 1000 s component providing the largest contribution. The settling behavior of the devices occurs in both ambient air and vacuum conditions (5 × 10^{-4} Torr), as shown in Figure S13, indicating that the majority of trap states are contributed by the substrate,[44] adsorbed water,[45] or a source separate from the ambient air. Consistent with other works, we observed a threshold voltage shift between air and vacuum conditions, likely due to the effect of removing oxygen gas from the environment.[29]

DOI: 10.1021/acs.nanolett.8b03986
Nano Lett. 2019, 19, 1460−1466

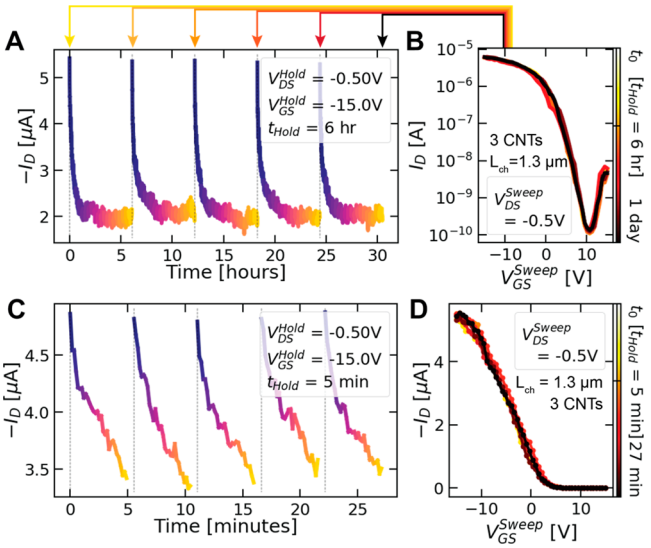

Figure 3. Reset of drain current settling by periodic gate voltage sweeps. (A) Repeated CNTFET drain-current settling during static bias intervals of 6 h. Intervals are interspersed by (B) 30 s gate sweeps that reveal the stability of CNTFET characteristics over time. (C) Drain-current settling curves with intervals of 5 min show a 30% reduction in current, but (D) transfer characteristics taken between intervals still show no change in the on-state performance.

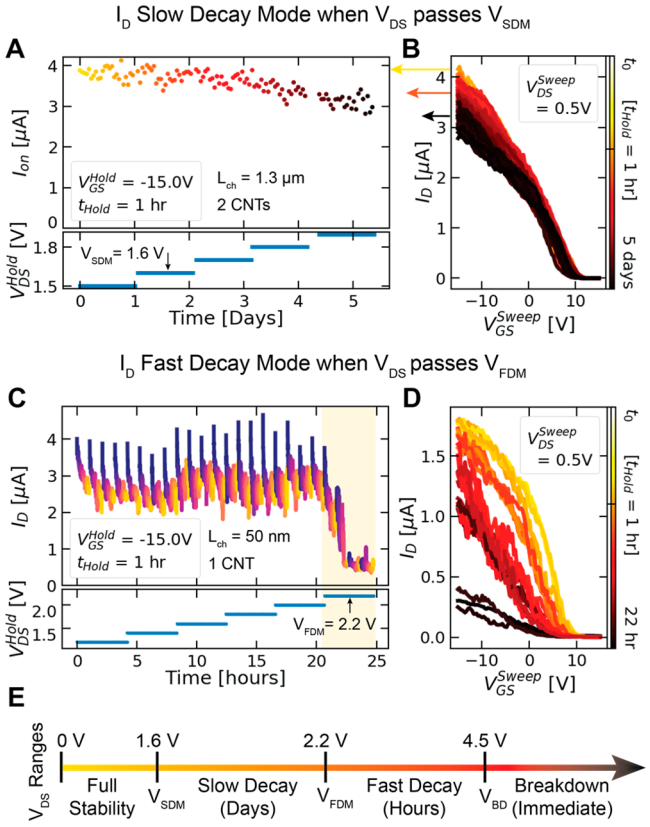

Figure 4. Slow and fast decay modes of CNTs at increasing bias. (A) Hourly measurements of on-current at V_{DS}^{Sweep} = 0.5 V revealing slow decay. Gate sweeps were performed hourly, in between intervals of static bias with V_{DS}^{Hold} increased by 0.1 V at the end of each day. (B) Transfer curves from the hourly gate sweeps, measured over 5 days. (C) Continuous drain-current measurements revealing fast decay (with gate sweeps taken hourly, causing the reset behavior). V_{DS}^{Hold} was incremented more aggressively, and decay occurred over the course of hours instead of days. (D) Transfer curves of the device demonstrating an initial slow decay and then sudden fast decay after $V_{DS}^{Hold} > V_{FDM}$. (E) Summary of operation modes and relevant voltage thresholds for a CNT with a 50 nm channel length.

Having confirmed CNTFET stability under moderate bias ($|V_{DS}^{Hold}| \leq 0.5$ V), the impact of increasing V_{DS} was explored. Consistent with previous work,[28,39,46] we observed an upper limit breakdown voltage (V_{BD}) beyond which the devices would fail immediately due to joule heating. To determine what other degradation may occur prior to breakdown, we incrementally increased V_{DS}^{Hold} after several static bias intervals. An unanticipated effect of the increasing bias stress were two distinct, irreversible decay modes for the nanotube current. The gradual decay observed in Figure 4A occurred over time scales of days with a steady decline in overall on-state characteristics (Figure 4B). The on-current (I_{on}) in Figure 4A is the drain current at V_{DS}^{Sweep} = 0.5 V and V_{GS}^{Sweep} = −15 V, collected from transfer curves measured after every t_{Hold} (1 h) of static bias. This slow decay mode has an onset voltage of V_{SDM}: when $V_{DS}^{Hold} \geq V_{SDM}$ and the CNT has been under bias stress for many hours, the decay begins to occur. For the device in Figures 4A and B, I_{on} decayed by ∼25% over 5 days, with a change in the static bias V_{DS}^{Hold} of only 0.4 V, with the majority of the current reduction occurring at high carrier concentrations (Figure S14). Further evidence of stability below V_{SDM} and slow decay above this threshold is provided in Figure S15.

Increasing V_{DS}^{Hold} well beyond V_{SDM} was found to result in a distinct change in the decay rate, characterized by a drop in I_{on} by more than an order of magnitude in a few hours. This fast decay mode has an onset voltage of V_{FDM} (Figures 4C and D), which was 2.2 V, still over 2 V below the breakdown voltage. Decay on similar time scales have been observed in multiwalled nanotubes,[38] but a different mechanism may be at play here. Eventually, when V_{DS}^{Hold} reached V_{BD} = 4.9 V, the nanotube experienced complete breakdown.

Four distinct ranges of device operation, determined by the applied V_{DS}, have been identified (Figure 4E). As long as V_{DS} is below V_{SDM}, the CNTFETs demonstrated full stability with no significant degradation over time. Above V_{SDM}, slow decay in on-state performance occurs with ∼5% loss per day. Beyond V_{FDM}, the devices enter fast decay, decreasing performance by approximately 43% per hour. Finally, if V_{DS} approaches V_{BD}, the device is in danger of immediate failure. These onset voltages vary somewhat from device to device but will most likely depend on channel length in a manner similar to that observed previously for the breakdown voltage.[28] In contrast to the reversible effects of trap filling observed with $V_{DS} < V_{SDM}$, the reduction in on-current seen in each of these decay modes is permanent.

The sensitivity of many CNTFET-based sensors increases with the dynamic range of its drain current modulated by the gate field, with some change in the vicinity of the CNT causing the modulation. The impact of different static bias conditions on this dynamic sensing range (especially based on the trap-related settling behavior from Figures 2 and 3) is explored in Figure 5. Drain current trends were measured in hour-long intervals, each at a unique V_{GS}^{Hold}, interspersed by gate voltage sweeps in the manner discussed previously (Figure S16). In Figure 5A, the color of the plotted drain current changes from blue to orange across each hour-long interval. Changes in V_{GS}^{Hold}

DOI: 10.1021/acs.nanolett.8b03986
Nano Lett. 2019, 19, 1460−1466

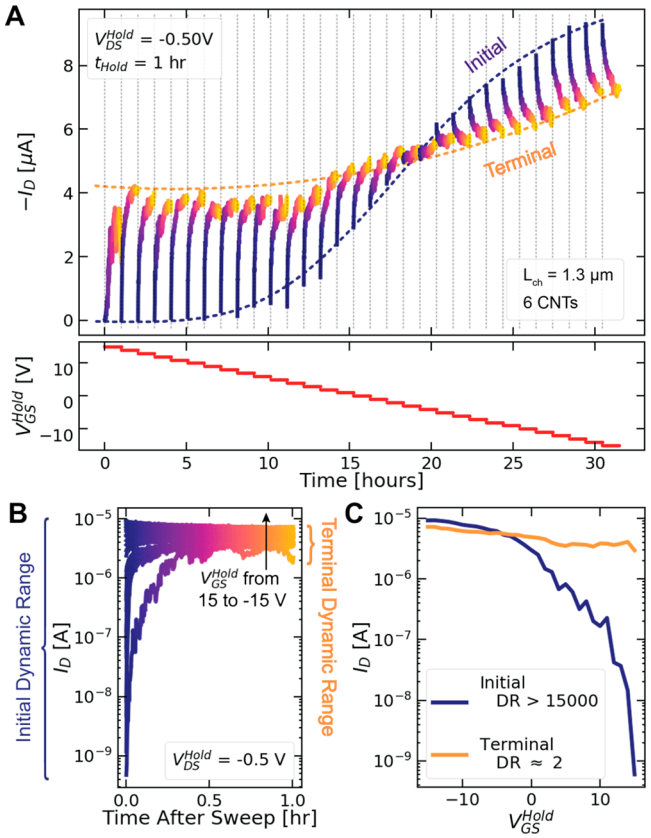

Figure 5. Loss of dynamic range during periods of static bias. (A) Monitoring drain current over hour-long static bias intervals with V_{GS}^{Hold} incremented each interval. Charge traps cause current to drift toward a common "Terminal" value regardless of applied gate field or "Initial" current. (B) Another view of the same data, plotting each data set from panel A in the same window with log-scale drain-current axis, revealing substantial reduction in dynamic range over time. (C) Extracted comparison of initial and terminal sensor response shows reduction in responsiveness to gating effects, which are the dominant transduction mode for many CNTFET-based sensors.

lead to different trap state occupancy conditions and thus different drain current settling behavior.

When V_{GS}^{Hold} is positive, the "initial" level of the drain current clearly resides in the CNTFET off-state; yet, over the course of the hour of static biasing, trapped charges cause the gate to lose control over the channel, leading to an increase in drain current over time. In short, the positive applied gate field is gradually filling traps with electrons, which are in turn gating the nanotube into the on-state. In fact, regardless of the initial drain current value, it drifts over time toward a common value, controlled by the charge traps. Thus, the range of initial current is much wider than the range of terminal current (Figure 5B), indicating a substantial decrease in dynamic range over time when the device is subjected to static bias conditions, and a much less favorable effective device response after time has elapsed in the static bias state (Figure 5C).

To interpret the span of drain current values as the dynamic range of a sensor, as suggested in Figure 5b, we must consider that what is ultimately being sensed in this data set is the static gate bias, V_{GS}^{Hold}. Along those lines, we may consider V_{GS}^{Hold} to be a simulation of the effect of an analyte. This stands to reason if CNTFET sensors function by analytes inducing an electrostatic gating effect, similar to V_{GS}^{Hold}. Although there are several mechanisms by which CNT-based sensors can function,[47] many derive their sensitivity from electrostatic gating effects.[18] Based on Figure 5C, the hour spent monitoring drain current reduces the dynamic range from electrostatic gating by 4 orders of magnitude, transforming the response curve into a nearly flat line. This is of significant import for the multitude of such sensors dependent on electrostatic gate-induced sensing.

These results suggest that in order to maintain high sensitivity and dynamic range, CNTFET-based sensors should be operated by sweeping the control gate as frequently as possible to redistribute charge, allowing the analyte to retain strong electrostatic control over the channel. Nanotubes themselves offer sufficient stability under moderate bias conditions, even when operated for months at a time (Figure S17), making the proper consideration of charge traps the most important aspect for stabilizing a CNTFET-based sensor. When sweeping the gate bias over a range of values is not possible for a given sensing system, alternating the gate between two values (e.g., on/off or positive/negative) should be an effective alternative. Reducing the trap state density could also help, but trap states will always be present to some degree,[48−50] and often the sensing environment itself introduces traps that may be unavoidable,[29,45,51] making this proposed sensor operation approach of great significance.

In conclusion, we developed an electrical characterization platform that allowed for the long-term interrogation of CNTFETs under various bias conditions. Four distinct operational modes were identified based on applied drain-source bias, wherein devices held at sufficiently low voltage exhibited stability for months of continuous operation. As applied bias increases beyond the full stability range, CNTs experience irreversible slow and then fast decay until eventually breaking down. The influence of charge traps—a known challenge for CNT-based devices of nearly every type—on the long-term electrical stability was also identified, presenting a reversible settling effect on the current. It was shown that this settling effect has significant implications for the dynamic range of a CNTFET-based sensor that operates continuously under fixed bias conditions. There are strategies for dealing with this trap-induced settling to preserve the dynamic range in such devices. Ultimately, these results describe what behaviors are to be expected when CNTs are stressed by continuous and variable biases over long periods of time and demark conditions under which the CNTs are electrically stable, providing valuable insight for the further advancement of the thousands of diverse CNTFET-based sensors that have been proposed.

■ ASSOCIATED CONTENT

Supporting Information

The Supporting Information is available free of charge on the ACS Publications website at DOI: 10.1021/acs.nanolett.8b03986.

Expanded materials and methods and supporting figures S1−S14 (PDF)

■ AUTHOR INFORMATION

Corresponding Author

*E-mail: aaron.franklin@duke.edu.

ORCID

Steven G. Noyce: 0000-0002-2953-7560

Aaron D. Franklin: 0000-0002-1128-9327

DOI: 10.1021/acs.nanolett.8b03986
Nano Lett. 2019, 19, 1460−1466

Author Contributions

S.N. and A.F. conceived the experiments. S.N. designed and fabricated the devices and designed and assembled the circuit boards. J.D. and S.N. wrote automation code and collected data; all authors aided in analyzing the approach and interpreting the results. S.N., J.D., and A.F. wrote the manuscript with input from all authors.

Funding

Supported by Illumina, Inc. under a sponsored research agreement. This work was performed in part at the Duke University Shared Materials Instrumentation Facility (SMIF), a member of the North Carolina Research Triangle Nanotechnology Network (RTNN), which is supported by the National Science Foundation (Grant ECCS-1542015) as part of the National Nanotechnology Coordinated Infrastructure (NNCI).

Notes

The authors declare no competing financial interest.

■ ACKNOWLEDGMENTS

We thank Greg Pitner and Philip Wong (Stanford University) for providing samples of CNTs on quartz substrates.

■ REFERENCES

(1) Tans, S.; Verschueren, A.; Dekker, C. Room-Temperature Transistor Based on a Single Carbon Nanotube. *Nature* **1998**, *393* (6680), 49−52.

(2) Yang, N.; Chen, X.; Ren, T.; Zhang, P.; Yang, D. Carbon Nanotube Based Biosensors. *Sens. Actuators, B* **2015**, *207* (PartA), 690−715.

(3) Martel, R.; Schmidt, T.; Shea, H. R.; Hertel, T.; Avouris, P. Single- and Multi-Wall Carbon Nanotube Field-Effect Transistors. *Appl. Phys. Lett.* **1998**, *73* (17), 2447−2449.

(4) Kauffman, D. R.; Star, A. Carbon Nanotube Gas and Vapor Sensors. *Angew. Chem., Int. Ed.* **2008**, *47* (35), 6550−6570.

(5) Peng, N.; Zhang, Q.; Chow, C. L.; Tan, O. K.; Marzari, N. Sensing Mechanisms for Carbon Nanotube Based NH 3 Gas Detection. *Nano Lett.* **2009**, *9* (4), 1626−1630.

(6) Someya, T.; Small, J.; Kim, P.; Nuckolls, C.; Yardley, J. T. Alcohol Vapor Sensors Based on Single-Walled Carbon Nanotube Field Effect Transistors. *Nano Lett.* **2003**, *3* (7), 877−881.

(7) Qi, P.; Vermesh, O.; Grecu, M.; Javey, A.; Wang, Q.; Dai, H.; Peng, S.; Cho, K. J. Toward Large Arrays of Multiplex Functionalized Carbon Nanotube Sensors for Highly Sensitive and Selective Molecular Detection. *Nano Lett.* **2003**, *3* (3), 347−351.

(8) Star, A.; Gabriel, J. C. P.; Bradley, K.; Grüner, G. Electronic Detection of Specific Protein Binding Using Nanotube FET Devices. *Nano Lett.* **2003**, *3* (4), 459−463.

(9) Maehashi, K.; Matsumoto, K. Label-Free Electrical Detection Using Carbon Nanotube-Based Biosensors. *Sensors* **2009**, *9*, 5368−5378.

(10) Byon, H. R.; Choi, H. C. Network Single-Walled Carbon Nanotube-Field Effect Transistors (SWNT-FETs) with Increased Schottky Contact Area for Highly Sensitive Biosensor Applications. *J. Am. Chem. Soc.* **2006**, *128* (7), 2188−2189.

(11) Maehashi, K.; Katsura, T.; Kerman, K.; Takamura, Y.; Matsumoto, K.; Tamiya, E. Label-Free Protein Biosensor Based on Aptamer-Modified Carbon Nanotube Field-Effect Transistors. *Anal. Chem.* **2007**, *79* (2), 782−787.

(12) Taupin, J. L.; Tian, Q.; Kedersha, N.; Robertson, M.; Anderson, P.; Li, Y.; Kim, W.; Utz, P. J.; Dai, H. The RNA-Binding Protein TIAR Is Translocated from the Nucleus to the Cytoplasm during Fas-Mediated Apoptotic Cell Death. *Proc. Natl. Acad. Sci. U. S. A.* **1995**, *92* (5), 1629−1633.

(13) Oh, J.; Yoo, G.; Chang, Y. W.; Kim, H. J.; Jose, J.; Kim, E.; Pyun, J. C.; Yoo, K. H. A Carbon Nanotube Metal Semiconductor Field Effect Transistor-Based Biosensor for Detection of Amyloid-Beta in Human Serum. *Biosens. Bioelectron.* **2013**, *50*, 345−350.

(14) Villamizar, R. A.; Maroto, A.; Rius, F. X.; Inza, I.; Figueras, M. J. Fast Detection of Salmonella Infantis with Carbon Nanotube Field Effect Transistors. *Biosens. Bioelectron.* **2008**, *24* (2), 279−283.

(15) Cid, C. C.; Riu, J.; Maroto, A.; Rius, F. X. Carbon Nanotube Field Effect Transistors for the Fast and Selective Detection of Human Immunoglobulin G. *Analyst* **2008**, *133* (8), 1005−1008.

(16) Besteman, K.; Lee, J.-O. O.; Wiertz, F. G. M. M.; Heering, H. A.; Dekker, C. Enzyme-Coated Carbon Nanotubes as Single-Molecule Biosensors. *Nano Lett.* **2003**, *3* (6), 727−730.

(17) Pugliese, K. M.; Tolga Gul, O.; Choi, Y.; Olsen, T. J.; Sims, P. C.; Collins, P. G.; Weiss, G. A. Processive Incorporation of Deoxynucleoside Triphosphate Analogs by Single-Molecule DNA Polymerase i (Klenow Fragment) Nanocircuits. *J. Am. Chem. Soc.* **2015**, *137* (30), 9587−9594.

(18) Choi, Y.; Olsen, T. J.; Sims, P. C.; Moody, I. S.; Corso, B. L.; Dang, M. N.; Weiss, G. A.; Collins, P. G. Dissecting Single-Molecule Signal Transduction in Carbon Nanotube Circuits with Protein Engineering. *Nano Lett.* **2013**, *13* (2), 625−631.

(19) Sorgenfrei, S.; Chiu, C. Y.; Gonzalez, R. L., Jr.; Yu, Y. J.; Kim, P.; Nuckolls, C.; Shepard, K. L. Label-Free Single-Molecule Detection of DNA-Hybridization Kinetics with a Carbon Nanotube Field-Effect Transistor. *Nat. Nanotechnol.* **2011**, *6* (2), 126−132.

(20) Tang, X.; Bansaruntip, S.; Nakayama, N.; Yenilmez, E.; Chang, Y. I.; Wang, Q. Carbon Nanotube DNA Sensor and Sensing Mechanism. *Nano Lett.* **2006**, *6* (8), 1632−1636.

(21) Xuan, C. T.; Thuy, N. T.; Luyen, T. T.; Huyen, T. T. T.; Tuan, M. A. Carbon Nanotube Field-Effect Transistor for DNA Sensing. *J. Electron. Mater.* **2017**, *46* (6), 3507−3511.

(22) Guo, X.; Huang, L.; O'Brien, S.; Kim, P.; Nuckolls, C. Directing and Sensing Changes in Molecular Conformation on Individual Carbon Nanotube Field Effect Transistors. *J. Am. Chem. Soc.* **2005**, *127* (43), 15045−15047.

(23) Bouilly, D.; Hon, J.; Daly, N. S.; Trocchia, S.; Vernick, S.; Yu, J.; Warren, S.; Wu, Y.; Gonzalez, R. L.; Shepard, K. L.; et al. Single-Molecule Reaction Chemistry in Patterned Nanowells. *Nano Lett.* **2016**, *16* (7), 4679−4685.

(24) Lee, S. W.; Lee, S. Y.; Lim, S. C.; Kwon, Y. D.; Yoon, J. S.; Uh, K.; Lee, Y. H. Positive Gate Bias Stress Instability of Carbon Nanotube Thin Film Transistors. *Appl. Phys. Lett.* **2012**, *101* (5), 053504.

(25) Lee, S. W.; Suh, D.; Lee, S. Y.; Lee, Y. H. Passivation Effect on Gate-Bias Stress Instability of Carbon Nanotube Thin Film Transistors. *Appl. Phys. Lett.* **2014**, *104* (16), 163506.

(26) Bargaoui, Y.; Troudi, M.; Bondavalli, P.; Sghaier, N. Gate Bias Stress Effect in Single-Walled Carbon Nanotubes Field-Effect-Transistors. *Diamond Relat. Mater.* **2018**, *84* (2017), 62−65.

(27) Wang, H.; Cobb, B.; Van Breemen, A.; Gelinck, G.; Bao, Z. Highly Stable Carbon Nanotube Top-Gate Transistors with Tunable Threshold Voltage. *Adv. Mater.* **2014**, *26* (26), 4588−4593.

(28) Pop, E. The Role of Electrical and Thermal Contact Resistance for Joule Breakdown of Single-Wall Carbon Nanotubes. *Nanotechnology* **2008**, *19* (29), 295202.

(29) Lin, H.; Tiwari, S. Localized Charge Trapping Due to Adsorption in Nanotube Field-Effect Transistor and Its Field-Mediated Transport. *Appl. Phys. Lett.* **2006**, *89* (7), 073507.

(30) Goldsmith, B. R.; Coroneus, J. G.; Kane, A. A.; Weiss, G. A.; Collins, P. G. Monitoring Single-Molecule Reactivity on a Carbon Nanotube. *Nano Lett.* **2008**, *8* (1), 189−194.

(31) Helbling, T.; Hierold, C.; Roman, C.; Durrer, L.; Mattmann, M.; Bright, V. M. Long Term Investigations of Carbon Nanotube Transistors Encapsulated by Atomic-Layer-Deposited Al2O3 for Sensor Applications. *Nanotechnology* **2009**, *20* (43), 434010.

(32) Peng, N.; Zhang, Q.; Yuan, S.; Li, H.; Tian, J.; Chan, L. Current Instability of Carbon Nanotube Field Effect Transistors. *Nanotechnology* **2007**, *18* (42), 424035.

(33) Franklin, A. D.; Tulevski, G. S.; Han, S. J.; Shahrjerdi, D.; Cao, Q.; Chen, H. Y.; Wong, H. S. P.; Haensch, W. Variability in Carbon

DOI: 10.1021/acs.nanolett.8b03986
Nano Lett. 2019, 19, 1460−1466

Nanotube Transistors: Improving Device-to-Device Consistency. *ACS Nano* **2012**, *6* (2), 1109−1115.
(34) Cannon, D. W.; Magee, D. P.; Book, W. J.; Lew, J. Y. Experimental Study on Micro/Macro Manipulator Vibration Control. *Robot. Autom. 1996. Proceedings., 1996 IEEE Int. Conf.* **1996**, *3*, 2549−2554.
(35) Kang, S. J.; Kocabas, C.; Ozel, T.; Shim, M.; Pimparkar, N.; Alam, M. A.; Rotkin, S. V.; Rogers, J. A. High-Performance Electronics Using Dense, Perfectly Aligned Arrays of Single-Walled Carbon Nanotubes. *Nat. Nanotechnol.* **2007**, *2* (4), 230−236.
(36) Kocabas, C.; Kang, S. J.; Ozel, T.; Shim, M.; Rogers, J. A. Improved Synthesis of Aligned Arrays of Single-Walled Carbon Nanotubes and Their Implementation in Thin Film Type Transistors. *J. Phys. Chem. C* **2007**, *111* (48), 17879−17886.
(37) Shulaker, M. M.; Wei, H.; Patil, N.; Provine, J.; Chen, H. Y.; Wong, H.-S. S. P.; Mitra, S. Linear Increases in Carbon Nanotube Density through Multiple Transfer Technique. *Nano Lett.* **2011**, *11* (5), 1881−1886.
(38) Mølhave, K.; Gudnason, S. B.; Pedersen, A. T.; Clausen, C. H.; Horsewell, A.; Bøggild, P. Transmission Electron Microscopy Study of Individual Carbon Nanotube Breakdown Caused by Joule Heating in Air. *Nano Lett.* **2006**, *6* (8), 1663−1668.
(39) Collins, P. G.; Arnold, M. S.; Avouris, P. Engineering Carbon Nanotubes and Nanotube Circuits Using Electrical Breakdown. *Science (Washington, DC, U. S.)* **2001**, *292* (5517), 706−709.
(40) Zhang, Y.; Iijima, S. Elastic Response of Carbon Nanotube Bundles to Visible Light. *Phys. Rev. Lett.* **1999**, *82* (17), 3472−3475.
(41) Pop, E.; Mann, D.; Wang, Q.; Goodson, K.; Dai, H. Thermal Conductance of an Individual Single-Wall Carbon Nanotube above Room Temperature. *Nano Lett.* **2006**, *6* (1), 96−100.
(42) Mattmann, M.; Roman, C.; Helbling, T.; Bechstein, D.; Durrer, L.; Pohle, R.; Fleischer, M.; Hierold, C. Pulsed Gate Sweep Strategies for Hysteresis Reduction in Carbon Nanotube Transistors for Low Concentration NO2 Gas Detection. *Nanotechnology* **2010**, *21* (18), 185501.
(43) Cao, Q.; Han, S. J.; Penumatcha, A. V.; Frank, M. M.; Tulevski, G. S.; Tersoff, J.; Haensch, W. E. Origins and Characteristics of the Threshold Voltage Variability of Quasiballistic Single-Walled Carbon Nanotube Field-Effect Transistors. *ACS Nano* **2015**, *9* (2), 1936−1944.
(44) Muoth, M.; Helbling, T.; Durrer, L.; Lee, S.-W.; Roman, C.; Hierold, C. Hysteresis-Free Operation of Suspended Carbon Nanotube Transistors. *Nat. Nanotechnol.* **2010**, *5* (8), 589−592.
(45) Kim, W.; Javey, A.; Vermesh, O.; Wang, Q.; Li, Y.; Dai, H. Hysteresis Caused by Water Molecules in Carbon Nanotube Field-Effect Transistors. *Nano Lett.* **2003**, *3* (2), 193−198.
(46) Shekhar, S.; Erementchouk, M.; Leuenberger, M. N.; Khondaker, S. I. Correlated Electrical Breakdown in Arrays of High Density Aligned Carbon Nanotubes. *Appl. Phys. Lett.* **2011**, *98* (24), 243121.
(47) Heller, I.; Janssens, A. M.; Mannik, J.; Minot, E. D.; Lemay, S. G.; Dekker, C. Identifying the Mechanism of Biosensing with Carbon Nanotube Transistors. *Nano Lett.* **2008**, *8* (2), 591−595.
(48) Kolodzey, J.; Chowdhury, E. A.; Adam, T. N.; Qui, G.; Rau, I.; Olowolafe, J. O.; Suehle, J. S.; Chen, Y. Electrical Conduction and Dielectric Breakdown in Aluminum Oxide Insulators on Silicon. *IEEE Trans. Electron Devices* **2000**, *47* (1), 121−128.
(49) DiMaria, D. J.; Cartier, E.; Arnold, D. Impact Ionization, Trap Creation, Degradation, and Breakdown in Silicon Dioxide Films on Silicon. *J. Appl. Phys.* **1993**, *73* (7), 3367−3384.
(50) Foster, A. S.; Lopez Gejo, F.; Shluger, A. L.; Nieminen, R. M. Vacancy and Interstitial Defects in Hafnia. *Phys. Rev. B: Condens. Matter Mater. Phys.* **2002**, *65* (17), 1741171−17411713.
(51) Collins, P. G.; Bradley, K.; Ishigami, M.; Zettl, A. Extreme Oxygen Sensitivity of Electronic Properties of Carbon Nanotubes. *Science (Washington, DC, U. S.)* **2000**, *287* (5459), 1801−1804.

DOI: 10.1021/acs.nanolett.8b03986
Nano Lett. 2019, 19, 1460−1466